J. Membrane Biol. 76, 289–297 (1983)

The Journal of
Membrane Biology

Characteristics of Manganese Current and Its Comparison with Currents Carried by Other Divalent Cations in Snail Soma Membranes

N. Akaike, K. Nishi* and Y. Oyama*

Department of Physiology, Kyushu University Faculty of Medicine, Fukuoka 812, and
* Department of Pharmacology, Kumamoto University Medical School, Kumamoto 860, Japan

Summary. Characteristics of currents carried by Mn^{2+} and other divalent cations were studied in the isolated identified neuron in the circumesophageal ganglia of *Helix aspersa* using a suction pipette technique which allows internal perfusion of the cell body and voltage clamp. Increases in $[Mn^{2+}]_o$ induced not only saturation of the peak of I_{Mn} but also shifts the *I–V* relationships along the voltage axis to the more positive potentials. Internal perfusion with F^-, which blocks Ca channels, depressed I_{Mn}. Diltiazem, an organic Ca blocker, inhibited I_{Mn} over the entire range of the *I–V* relation without shifting the threshold and peak voltage of the *I–V* relation. Co^{2+}, Ni^{2+}, Cd^{2+} and La^{3+} also suppressed I_{Mn}. Relative maximum peak currents of the divalent cations were $I_{Ba}=I_{Sr}>I_{Ca}>I_{Mn}=I_{Zn}$. Time constants for activation (τ_m) and inactivation (τ_h) of these cations were voltage dependent, and both time constants were greater in the sequence of $I_{Mn}=I_{Zn}>I_{Ba}=I_{Sr}>I_{Ca}$ over the whole voltage range.

Key Words neuron · internal perfusion · Mn current · kinetics · Ca blocker

Introduction

The transition metal divalent cations (Mn^{2+}, Co^{2+}, Fe^{2+}, Zn^{2+} and Ni^{2+}) reduce the Ca^{2+} inward current (I_{Ca}) in barnacle muscle (Hagiwara & Takahashi, 1967*a*) and molluscan neurons (Geduldig & Gruener, 1970; Kostyuk, Krishtal & Shakhovalov, 1977; Akaike, Lee & Brown, 1978; Akaike et al., 1978; Adams & Gage, 1979; Akaike et al., 1981) by competing with Ca^{2+} for a common receptor site of the Ca channel in a concentration-dependent manner. In the absence of Ca^{2+} in the external medium, however, several divalent cations, such as Mn^{2+}, Zn^{2+}, Cd^{2+} and Ba^{2+}, have been shown to carry small amounts of current across the plasma cell membrane (Yamagishi, 1973; Kawa, 1979; Akaike, Nishi & Oyama, 1981; Oyama et al., 1982). Among these divalent cations, currents carried by Mn^{2+} have been studied in various tissues and organs. Marine worm epithelial cells (Anderson, 1979) and larval beetle muscle (Fukuda & Kawa, 1977) immersed in Ca^{2+}-free solutions containing various concentrations of Mn^{2+} have action potentials whose overshoot and maximum rate of rise increase with increased external Mn^{2+} concentrations. A voltage-dependent influx of Mn^{2+} through the 'Ca channels' has been also reported in guinea pig cardiac muscle (Ochi, 1970; 1976), mouse oocytes (Okamoto, Takahashi & Yamashita, 1977), starfish eggs (Hagiwara & Miyazaki, 1977) and frog skeletal muscle (Palade & Almers, 1978). At this moment, however, the voltage dependence, kinetics and pharmacological characteristics of the Mn^{2+} inward current (I_{Mn}) are not well understood since the study on I_{Mn} suffers from complications arising from the difficulty in separating pure I_{Mn} from other ionic currents. However, this difficulty has been overcome recently by application of a suction pipette technique which combines internal perfusion of the cell body with voltage clamp. This technique has been successfully utilized to analyze Ca^{2+} currents in *Helix* neurons (Akaike, 1980; Lee, Akaike & Brown, 1980). The aim of the present experiments is to characterize I_{Mn} with respect to the electrical and pharmacological properties in the identified single nerve cell body of *Helix* neurons, utilizing the suction pipette technique, and to obtain further information about properties of Ca channels in the *Helix* neuron by comparing I_{Mn} with currents carried by other divalent cations.

A preliminary account of some of these results has been presented to the Hawaii Meeting about Gated Calcium Transport (Akaike, Nishi & Oyama, 1981).

Materials and Methods

All experiments were performed on the largest identifiable neuron of about 150 μm in diameter (F-1 cell, Kerkut et al., 1975) isolated from the subesophageal ganglia of *Helix aspersa*. The

Table 1. Ionic composition of standard Mn^{2+} Ringer's solution (mM)

External		Internal	
Tris-Cl	35	Cs-aspartate	135
CsCl	5	TEA-OH	10
$MnCl_2$	25	EGTA	0.1
TEA-Cl	50		
glucose	5.5		
4-AP	5		
pH 7.2 to 7.3		pH 7.4	

Changes of $[Mn^{2+}]_o$ were made by replacing the Mn^{2+} with Mg^{2+}, $Tris^+$ and/or TEA^+ according to the experimental conditions. I_{Ca}, I_{Ba}, I_{Sr} and I_{Zn} were obtained by the equimolar substitution of Ca^{2+}, Ba^{2+}, Sr^{2+} and Zn^{2+} for Mn^{2+}. The external test solution containing Zn^{2+} was adjusted to pH 6.8. The pH of all external solutions were adjusted with 5 mM Hepes

ganglion was removed and the connective tissue was stripped off with fine forceps. A part of the soma membrane was aspirated into a suction pipette having tip interior diameter of 20 to 22 μm and then the neuron pulled free of neighboring cells and its axon. A suction pipette method was used for voltage-clamp and internal perfusion (Akaike, 1980; Lee et al., 1980). An additional glass microelectrode, filled with 3 M CsCl and having a resistance of about 1.5 to 1.8 MΩ was used to record membrane potential which was summed with the command step during voltage clamping. The leakage current is defined as a remaining current after blocking I_{Mn} by Co^{2+} and has linear and nonlinear components. The linear residual currents along with the linear portion of the capacitative current transient were subtracted by adding the current responses to equal and opposite voltage steps. Nonlinear leakage current (I_{NS}) was evaluated separately. The command potentials rose with a time constant of 20 to 35 μsec. The capacitative current transient relaxed with a single time constant of 250 to 300 μsec. The membrane capacitance, C_m, was estimated from the time constant of the monoexponential hyperpolarizing or depolarizing potential change produced by an inward or outward step of current. The estimated C_m of F-1 cell was about 3 to 4×10^{-9} F.

The Ca^{2+} current (I_{Ca}) was segregated by suppressing Na^+ and K^+ currents (I_{Na} and I_K, respectively). I_{Na} was suppressed by substitution of $Tris^+$ for Na^+ in external solution. I_K was suppressed by substituting Cs^+ for K^+ in both external and internal solutions and adding TEA^+ to both the solutions (Akaike, Lee & Brown, 1978). 4-aminopyridine (4-AP) was added to the external solution to block a transient K^+ current (I_A) (Connor & Stevens, 1971; Thompson, 1977). In experiments for analyzing currents carried by Ba^{2+}, Sr^{2+}, Mn^{2+} and Zn^{2+}, the Ca^{2+} in the test solutions was replaced with an equimolar concentration of the divalent ion under study. Compositions of the test solutions are given in the Table. The test solutions for I_{Ca}, I_{Ba}, I_{Sr} and I_{Mn} were adjusted at pH 7.2 to 7.3, and the solution for I_{Zn} at pH 6.8.

Ionic currents were monitored on a storage oscilloscope (Tektronix 5113), and simultaneously recorded with a photosensitive paper recorder system (Medelec, MS6) and stored on a digital tape recorder (Kennedy 9700C). The linear components of the transient capacitative and leakage currents associated with the ionic currents were subtracted during the experiments by adding the current response to equal but opposite voltage steps using a signal averager (Nihon Kohden, ATAC-150).

The organic Ca^{2+} blocker, diltiazem, was dissolved in test solution just before use. Unless otherwise stated, test solutions were made up from refrigerated stock solutions.

All experiments were done at room temperatures of 20 to 23° C.

Results

Mn^{2+}-Dependent Action Potenitals

After the neuron was separated from its axon in the normal solution, the preparation was exposed to Na^+- and K^+-free external and internal solutions for 10 to 15 min, after which complete blockage of Na^+ and K^+ currents (I_{Na} and I_K, respectively) occurred. Thereafter, Ca^{2+} in the external medium was replaced with equimolar Mn^{2+}. Within a few minutes after exposure to the Mn^{2+} solution, the soma membrane hyperpolarized slightly and all-or-none action potentials lasting for more than 10 to 20 sec could be evoked by a stimulus voltage beyond the threshold level (Fig. 1*A*). Increases in the external Mn^{2+} concentration ($[Mn^{2+}]_o$) did not alter significantly the resting membrane potential, but the Mn^{2+}-dependent action potentials required higher stimulus currents than Ca^{2+} action potentials. The amplitude and maximum rate of rise of the action potentials depended on $[Mn^{2+}]_o$ within the range of 5 and 50 mM, and the overshoot increased by 23 to 27 mV with a tenfold increase in $[Mn^{2+}]_o$. These results suggest that the inward current responsible for the action potentials is due to an increase in the Mn^{2+} permeability. The Mn^{2+}-dependent action potentials were not depressed by 3×10^{-5} M tetrodotoxin, which was enough to block Na channels in *Helix* neurons (Lee, Akaike & Brown, 1977), but were markedly inhibited by organic and inorganic Ca^{2+} antagonists such as diltiazem, Co^{2+}, Ni^{2+}, Zn^{2+}, Cd^{2+} and La^{3+} at concentrations appropriate to block I_{Ca} in *Helix* neurons (Akaike et al., 1981).

Current-Voltage Characteristics of I_{Mn}

A slowly rising Mn^{2+} inward current (I_{Mn}) appeared at potentials 25 to 30 mV more positive than the holding potential (V_H) of −50 mV at an external Mn^{2+} concentration of 25 mM, rose smoothly, and reached its peak within 5 to 20 msec depending on amplitude of the depolarizing voltage steps. The current reached its peak more rapidly at larger depolarizing voltages, and the maximum peak current occurred at a membrane potential level of +25 to +30 mV (Fig. 1*B* & *C*). On applying more positive voltage steps beyond this

level, the inward peak current became smaller, flattened and finally reversed at potential levels beyond +80 to +90 mV (Fig. 1*C*). The outward current appearing at high voltages has been referred to as nonspecific outward current (I_{NS}) (Akaike, Lee & Brown, 1978; Akaike, Nishi & Oyama, 1981; Brown et al., 1981; Byerly & Hagiwara, 1982; Oyama et al., 1982). According to Brown et al. (1981), Co^{2+} has little effect on I_{NS} although is completely suppresses I_{Ca} of *Helix* neuron. Therefore, Co^{2+} substitution for Mn^{2+} extracellularly may also be the most specific and/or suitable method for ionic blockage of I_{Mn} in the present experiment. After substitution of Co^{2+} for Mn^{2+}, the I_{NS} began at voltages around +20 to +25 mV and became larger at more positive potentials. The activation process of the voltage-dependent I_{NS} was also time-dependent as shown in Fig. 6*B*. Hence, I_{Mn} recorded at high voltages was contaminated with the I_{NS}. The expected real current-voltage (*I–V*) relationship for I_{Mn} could be obtained after correction for I_{NS}. The *I–V* relationship for I_{Mn} thus obtained is illustrated in Fig. 1*C*, in which no outward current of I_{Mn} was observed even at high voltages. Almost zero current in the I_{Mn} *I–V* relationship was observed at about +140 mV. However, it should be pointed out that the subtraction shown in Fig. 1*C* might not be taken very seriously since the surface potential in 25 mM Co^{2+} probably is not the same as in 25 mM Mn^{2+}.

Effects of Changing $[Mn^{2+}]_o$ on I_{Mn}

The effects of increasing or decreasing $[Mn^{2+}]_o$ at various $[Mg^{2+}]_o$ were examined. Increases in $[Mn^{2+}]_o$ with $[Mg^{2+}]_o = 0$ produced a larger peak I_{Mn}, shifted both maximum peak and threshold voltages of the *I–V* relationship in the positive direction, and the null potential became more positive with increases in $[Mn^{2+}]_o$. In contrast, decreases in $[Mn^{2+}]_o$ induced smaller I_{Mn} and shifted the *I–V* curves to negative potentials (Fig. 2*A*). The maximum peak values of I_{Mn} at various $[Mn^{2+}]_o$ showed a hyperbolic relationship with $[Mn^{2+}]_o$ (Fig. 2*B*).

Saturation of I_{Ca} with increasing $[Ca^{2+}]_o$ has been reported in barnacle muscle (Hagiwara & Takahashi, 1967*b*), tunicate eggs (Okamoto, Takahashi & Yoshii, 1976) snail neurons (Akaike, Lee & Brown, 1978) and *Paramecium tetraurelia* (Satow & Kung, 1979). However, there is the possibility that the intrinsic relationship between I_{Ca} and $[Ca^{2+}]_o$ could be complicated with the stabilizing action of Ca^{2+} on the cell membrane, such as reported by Frankenhaeuser and Hodgkin (1957).

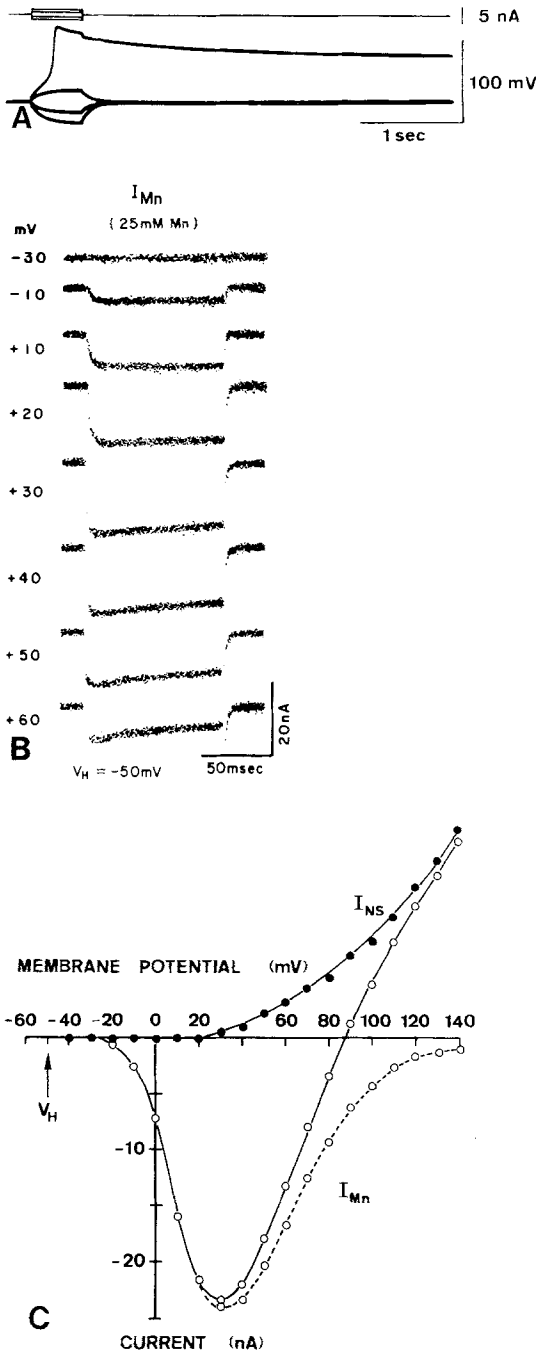

Fig. 1. Mn^{2+} action potential and inward currents. *A*. An all-or none action potential in Na^+-, K^+-, Mg^{2+}- and Ca^{2+}-free external solution containing 10 mM Mn^{2+} after complete blockage of Na^+ and K^+ channels. Note the prolonged plateau phase of the action potential. *B*. Inward currents obtained in Na^+-, K^+-, Mg^{2+}- and Ca^{2+}-free external solution containing 25 mM Mn^{2+}. The numbers at the left-hand side are the command voltage steps (mV) applied from the holding potential (V_H) of −50 mV. Sample records of I_{Mn} were obtained after subtraction of leakage and linear capacitive currents. *C*. Peak curves for the I_{Mn} (o) and the nonspecific outward current (I_{NS}) (•). After subtraction of I_{NS} for I_{Mn}, the real I_{Mn} *I–V* curve (o, broken line) was obtained. A reversal current of I_{Mn} was not observed after the subtraction. The inward currents became closer to zero at voltage steps higher than +120 mV

To avoid this complication, Hagiwara and Takahashi (1967*b*) studied the dependence of the I_{Ca} in barnacle muscle on $[Ca^{2+}]_o$ in solutions containing 100 mM Mg^{2+}, in which both the threshold and maximum rate of rise of action potentials remained constant at different $[Ca^{2+}]_o$. Therefore, in the present experiments, the dependence of I_{Mn} on $[Mn^{2+}]_o$ was examined according to the experimental protocol for the I_{Ca} in the barnacle muscle in the presence of high Mg^{2+} in the external medium as described above. Increasing the external Mg^{2+} concentrations from 0 to 40 mM reduced I_{Mn}. However, the shift of *I–V* relation for I_{Mn} was still observed, though the potential shift was reduced in the presence of 40 mM $[Mg^{2+}]_o$ (Fig. 2*B*).

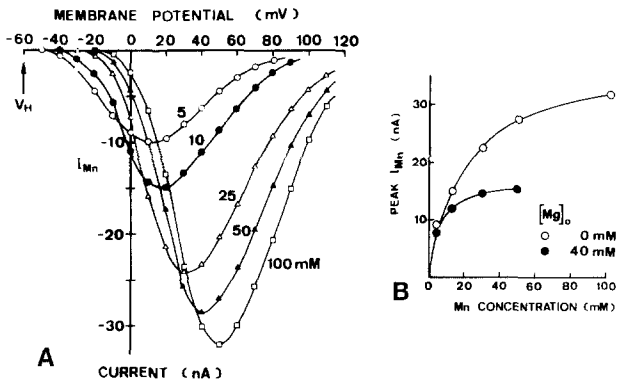

Fig. 2. I_{Mn} at various $[Mn^{2+}]_o$. *A.* I_{Mn} *I–V* relationship plotted as a function of $[Mn^{2+}]_o$. Each *I–V* curve was plotted 5 min after changing the external perfusate. Note the marked shifts of the current thresholds and peak voltages in the *I–V* relationships with increasing $[Mn^{2+}]_o$. $V_H = -60$ mV. *B.* Effects of changing $[Mn^{2+}]_o$ upon the maximum peak current in the *I–V* curves at each test solution with (○) and without (●) 40 mM Mg^{2+}. $V_H = -60$ mV. I_{Mn} increased in a hyperbolic manner as $[Mn^{2+}]_o$ was increased

Effects of Organic and Inorganic Ca^{2+} Antagonists on I_{Mn}

An organic Ca^{2+} antagonist, diltiazem, inhibited I_{Ca} of snail neurons in a dose-dependent manner (Akaike et al., 1981). In the present experiments, diltiazem slightly reduced I_{Mn} at a concentration of 5×10^{-6} M within 10 min, and further increases of drug concentration produced dose-dependent inhibition of I_{Mn}. The *I–V* relations for I_{Mn} before and after external application of diltiazem (5×10^{-5} M) for 10 min are shown in Fig. 3*A*. The Figure also shows the inhibitory effect of diltiazem applied internally at the same concentration for 10 min, though the inhibitory effect became almost equal to that of external application after 20 min internal perfusion. In addition, the internal diltiazem effect appeared within 3 min after the beginning of internal perfusion and the inhibition was reversible. When applied either externally or internally diltiazem depressed I_{Mn} without shifting the peak voltage of I_{Mn} in the *I–V* relationship.

La^{3+}, Ni^{2+}, Cd^{2+}, Mn^{2+} and Co^{2+} block I_{Ca} of *Helix* neurons in a dose-dependent manner (Akaike et al., 1981). Therefore, effects of these cations on I_{Mn} were studied. A typical example of the effects of Co^{2+} on I_{Mn} *I–V* relationship is shown in Fig. 3*B*. At 10 mM, Co^{2+} supressed I_{Mn} and shifted the *I–V* relationship slightly to more positive voltages. Similarly, 1 mM Ni^{2+}, Cd^{2+} and La^{3+} exerted inhibitory effects on I_{Mn} evoked in the presence of 25 mM Mn^{2+}, but these inhibitory actions were more potent than that of 10 mM Co^{2+} in inhibiting I_{Mn}.

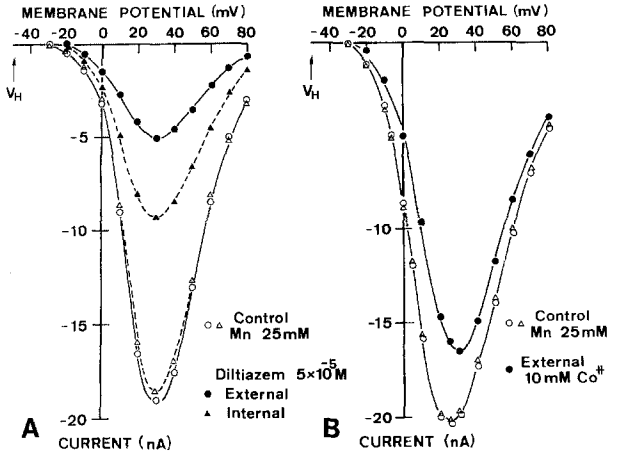

Fig. 3. Effects of diltiazem and Co^{2+} on I_{Mn} *I–V* curves. *A.* (○) control for the external application (●) of 5×10^{-5} M diltiazem on I_{Mn} evoked in solution containing 25 mM Mn^{2+}; (△) control for the internal application (▲) of 5×10^{-5} M diltiazem after complete washing out of the externally applied diltiazem. *B.* (○) control; (●) external application of 10 mM Co^{2+}; (△) recovery. *A* and *B* were obtained from different experiments

Internal Perfusion of F^-

Since it has been reported that internal application of F^- stabilized the cell membrane and blocks Ca channels in the *Helix* neuron (Kostyuk, Krishtal & Pidoplichko, 1975; Oyama et al., 1982) and unfertilized tunicate eggs (Takahashi & Yoshii, 1978), the effects of internal application of F^- on I_{Mn} were also examined. Cs-aspartate in the internal solution was replaced with equimolar CsF. After switching to a CsF test solution, both I_{Ca} and I_{Mn} were depressed gradually and abolished completely within 15 min (Fig. 4). The inhibitory action was irreversible. The results described so far provide evidence that the voltage-dependent Ca channel in the *Helix* neuron is permeable to Mn^{2+}.

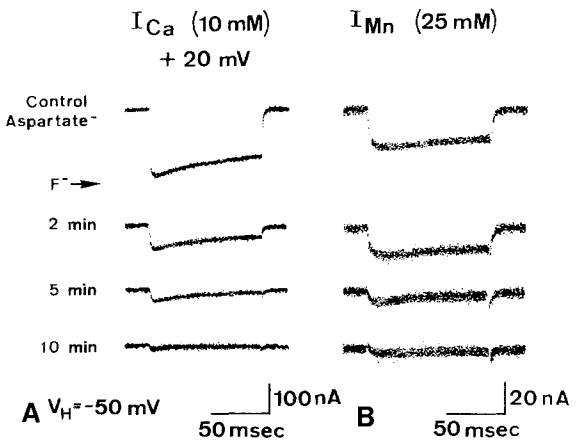

Fig. 4. *A*. Effect of internal perfusion of F^- on I_{Ca} evoked in external solution containing 10 mM Ca^{2+}. CsF was internally perfused. *B*. Effect of the internal application of F^- on I_{Mn} obtained in test solution containing 25 mM Mn^{2+}. *A* and *B* are obtained from different preparations. Numbers indicate the time after beginning of the internal perfusion. Note the change in current calibration in records, *A* and *B*

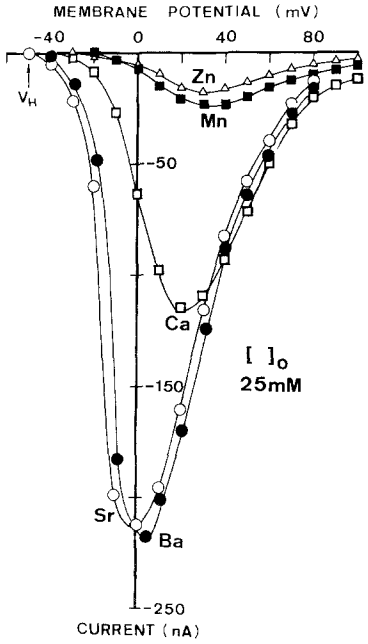

Fig. 5. *I–V* relationships of various divalent cations. I_{Ca} (□), I_{Ba} (●), I_{Sr} (○), I_{Mn} (■) and I_{Zn} (△) were recorded in Na^+-, K^+- and Mg^{2+}-free test solutions containing 25 mM of each divalent cation. Data were obtained from the same neuron. Note the shift of threshold and peak voltages in the *I–V* relationships among these different cations

Currents Carried by Other Divalent Cations

In the absence of Ca^{2+}, K^+ and Na^+ in the external and internal solutions, currents carried by Ba^{2+}, Sr^{2+} or Zn^{2+} were compared with I_{Mn} in the neuron. The preparations were exposed to test solutions containing each cation for 10 min, and then depolarizing voltage steps were applied so as to obtain *I–V* relationships for each ionic current. The *I–V* relations for each ionic current, thus obtained, were shifted along the voltage axis with respect to one another (Fig. 5). The sequence of potency was estimated from the amount of the voltage shift of the peak in each *I–V* relation and was $Mn^{2+} = Zn^{2+} > Cd^{2+} > Ba^{2+} = Sr^{2+}$. When the maximum peak inward currents carried by these cations were compared with the peak I_{Ca}, the average ratios of I_{Ba}, I_{Sr}, I_{Mn} and I_{Zn} to I_{Ca} were 1.8, 1.7, 0.2 and 0.17, respectively, at an external ionic concentration of 25 mM for each ion. Activation and inactivation processes of each ionic current took different time courses, which will be described later. In addition, I_{Ca} and I_{Ba} were reduced by about 15% by a one-half unit drop from pH 7.3 to 6.8 (*unpublished observation*).

Analysis of Activation and Inactivation of I_{Mn}

The peak voltage in the I_{Mn} *I–V* relationship shifted to more positive potentials in the absence than in the presence of Mg^{2+}. This voltage shift, presumably due to effects of Mn^{2+} on surface charge of the soma membrane, cannot be negligible for analyzing the true activation and inactivation processes of currents carried by Mn^{2+} and other divalent ions, since the voltage shift would produce and equivalent shift in the relationship between the activation and inactivation time constants and membrane potential. Therefore, all experiments analyzing activation and inactivation of currents carried by these divalent cations were done in cells immersed in test solutions containing 40 mM Mg^{2+}. Furthermore, as noted earlier in the text, the analyses of activation and inactivation kinetics were performed after the correction of recorded inward currents for I_{NS}, which is illustrated in Fig. 6.

The onset of I_{Mn} appeared with almost no delay and the successive rising phase showed no inflection. The time course of the activation of I_{Mn} was fitted by a single exponential function having a time constant refered to as τ_m using a Hodgkin-Huxley equation (1952). The τ_m for I_{Mn} declined with increases in the membrane potential, and the peak τ_m was about 20 msec at the membrane level of −10 mV. Values for τ_m and membrane potential for Mn^{2+}, Zn^{2+}, Sr^{2+}, Ba^{2+} and Ca^{2+}, obtained from a single same neuron, are shown in Fig. 8*A*. When compared with the τ_m for I_{Ca}, the values for both I_{Mn} and I_{Zn} were larger over the entire

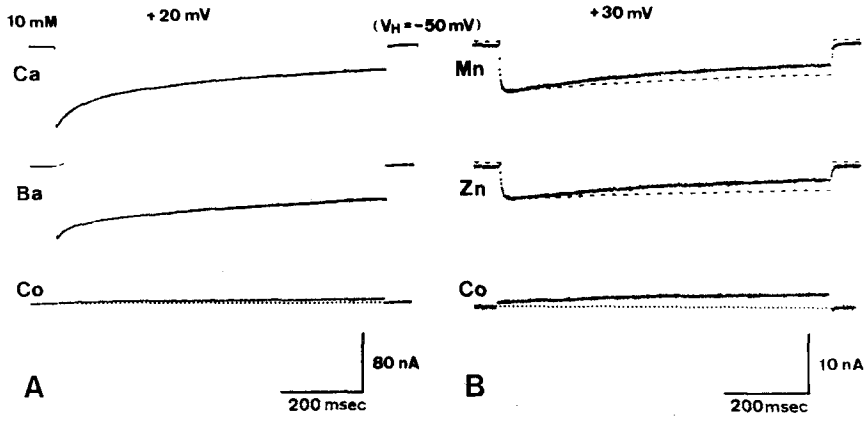

Fig. 6. The time courses of I_{Ca}, I_{Ba}, I_{Mn} and I_{Zn} currents. *A*. I_{Ca} and I_{Ba} generated by a pulse (800 msec duration) to +20 mV in Na^+-, K^+- and Mg^{2+}-free test solution containing 10 mM Ca^{2+} and Ba^{2+}, respectively. The current records were obtained after subtraction of leakage and capacitative currents. I_{NS} was obtained after substitution of Co^{2+} for Ca^{2+} and Ba^{2+}. *B*. I_{Mn} and I_{Zn} elicited by voltage steps to +30 mV. Traces of dotted lines in both I_{Mn} and I_{Zn} show the real currents after the correction for I_{NS}. Note the different current calibration in records in *A* and *B*

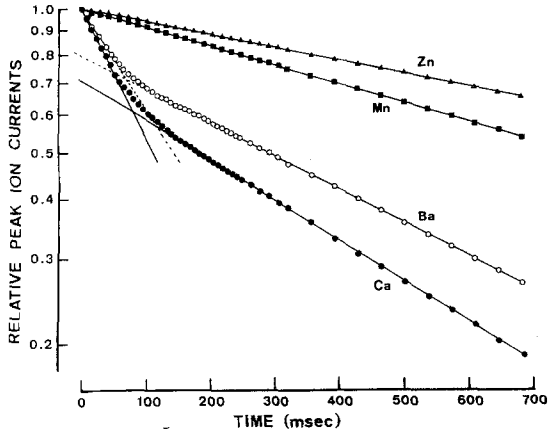

Fig. 7. Semilogarithmic plots of the time course of inactivation of I_{Ca}, I_{Ba}, I_{Mn} and I_{Zn}. I_{Ca} and I_{Ba} were elicited by voltage step to +20 mV while I_{Mn} and I_{Zn} to +30 mV. Leakage current, capacitative current and I_{NS} were subtracted. Data were obtained from records such as those in Fig. 6. Note a decay with a single component for I_{Mn} and I_{Zn} and two components for I_{Ca} and I_{Ba}

range of the membrane potential, and the τ_m for I_{Mn} was more voltage-dependent than that for I_{Ca} even at high voltages. On the other hand, τ_m values for I_{Sr} and I_{Ba} plotted against the membrane potential took different courses from those of I_{Mn}; at low voltages τ_m was relatively high, but beyond the membrane level of 0 to +10 mV, the values were almost the same as those of I_{Ca}. The peak τ_m for I_{Ca} was about 5 to 10 mV more positive than that for I_{Ba} and I_{Sr}, but less positive than those for I_{Mn} and I_{Zn}. Similar results were obtained using plots of the voltage dependence of the half-time of the rising phase of the inward currents.

It has been shown that inactivation of I_{Ca} and I_{Ba} is a biphasic process with fast and slow time constants, τ_{h1} and τ_{h2}, respectively (Magura, 1977; Kostyuk, 1980; Akaike, Nishi & Oyama, 1981; Brown et al., 1981). As shown in Fig. 7, I_{Ca}, I_{Ba} and I_{Sr} evoked by an 800 msec test pulse also inactivated slowly with a time course fitted by two exponential functions. However, the inactivation process of I_{Mn} and I_{Zn} occurred slowly at a rate which was fitted by a single exponential function, even for a depolarizing command pulse lasting for more than 2 sec. The τ_h declined steeply at the membrane level between −10 and +10 mV. Thus, the inactivation processes of I_{Mn} and I_{Zn} show voltage-dependency more than those of I_{Ca} and I_{Ba}. Furthermore, the τ_h for I_{Mn} was larger than τ_{h2} for I_{Ca} and I_{Ba} over the entire range of the membrane potential (Fig. 8*B*).

The Hodgkin-Huxley steady-state inactivation parameter (1952), $h\infty$, for I_{Mn} was measured as the ratio of test pulse current in the presence of a prepulse to test pulse current in the absence of the prepulse, and compared with $h\infty$ for I_{Ca} and I_{Ba}. Results are shown in Fig. 9*B*, where the duration of the prepulse was fixed to 3 sec and various voltage steps of the prepulse were applied. When prepulse potentials became positive, the peak amplitude of the test I_{Mn} was reduced, and reached the lowest value, about 50% of the control, at the membrane level of +30 mV. However, further increase in the amplitude of the prepulse did not produce a decrease in the peak test I_{Mn}. On the other hand, the test I_{Ca} was almost completely inactivated at about +30 mV and then started to increase at high positive potentials. The test I_{Ba} also decreased with increases in prepulse potentials to about 20% of the control at +30 mV and then increased at +50 mV. For considerable inactivation of the test I_{Ba}, long prepulses of 5 to 10 sec were required.

The $h\infty$–V relationships for I_{Mn} were examined at different durations of the prepulse. The values of $h\infty$ for I_{Mn} decreased with the prolongation of the prepulse, but a marked inactivation of the test I_{Mn} was not observed even with a prepulse duration

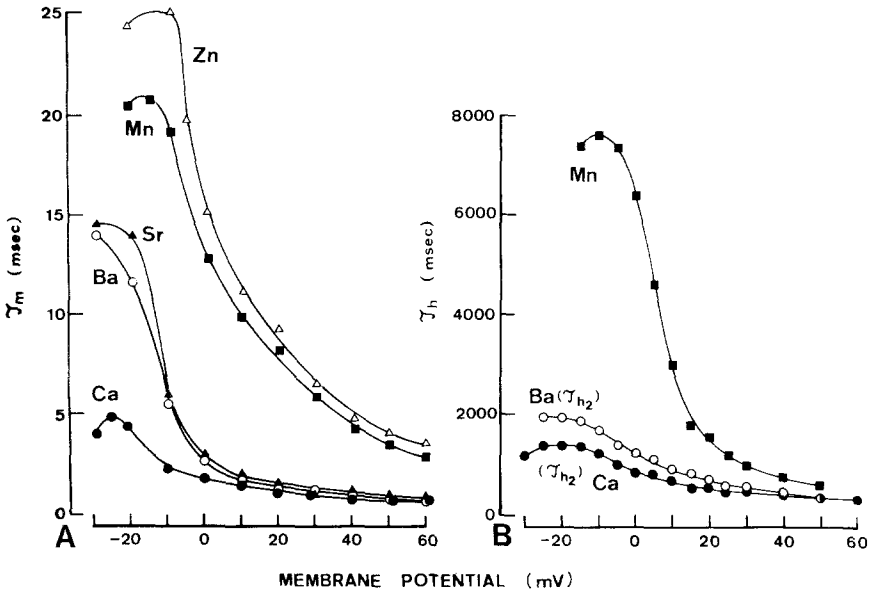

Fig. 8. Time constants for activation (τ_m) and inactivation (τ_h) of divalent inward currents as a function of membrane potential. Data were obtained from the same cell in 10 mM Ca^{2+}, Ba^{2+}, Sr^{2+}, Mn^{2+} and Zn^{2+} test solutions containing 40 mM Mg^{2+}. $V_H = -50$ mV. *A*. τ_m values of I_{Ca}, I_{Ba}, I_{Sr}, I_{Mn} and I_{Zn}. *B*. τ_h values of I_{Ca}, I_{Ba} and I_{Mn}

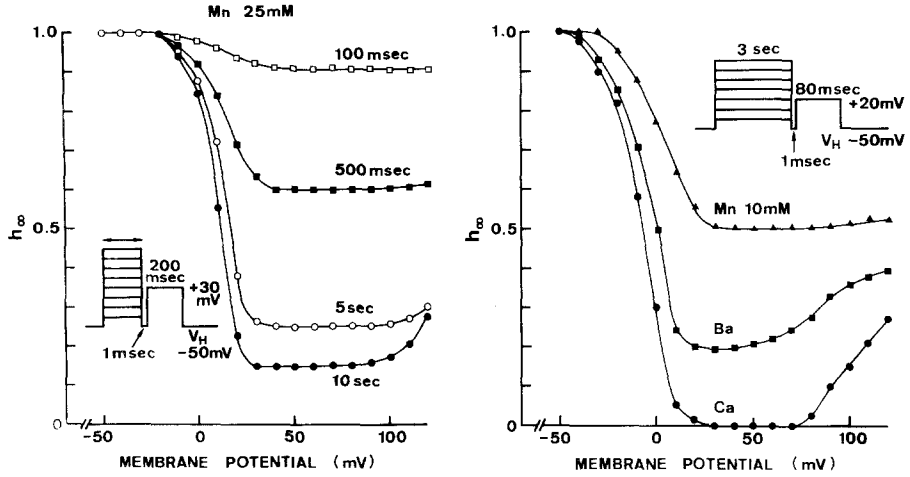

Fig. 9. Comparison of the inactivation parameter, $h\infty$, for I_{Ca}, I_{Ba} and I_{Mn} in the same neuron. There was an interval of 1 msec between the 'conditioning' prepulse and the test pulse, but this pause did not affect the results. *A*. I_{Mn} was not completely inactivated even at prepulse lasting for 10 sec. *B*. Note marked inactivation for I_{Ca}, but not for I_{Ba} and I_{Mn}

of 10 sec (Fig. 9*A*). The τ_h values together with the $h\infty$–V relationships for Ca^{2+}, Ba^{2+}, Sr^{2+}, Mn^{2+} and Zn^{2+} currents suggest that the order of inactivation of these currents is $I_{Ca} > I_{Ba} = I_{Sr} > I_{Mn} = I_{Zn}$.

Discussion

The present experiments have demonstrated that the soma membrane of *Helix* neuron can generate all-or-none action potentials in a solution in which the only permeable cation is Mn^{2+} in the absence of Na^+, K^+ and Ca^{2+} in the external and internal solutions, and that under voltage clamp conditions the inward currents induced by depolarizing voltage steps from the holding potential (V_H) of -50 mV are dependent on $[Mn^{2+}]_o$. The results indicate that the current is a 'Mn^{2+} current' through 'Ca channels.' The evidence to support this conclusion is: (1) The threshold voltage to initiate I_{Mn} is about -20 mV, which is close to the critical voltage level of eliciting I_{Ca} and less negative than the level to induce I_{Ca} through 'Na channels' in the egg cell membrane (Okamoto et al., 1976). (2) There was no reversal of I_{Mn} after correction of the recorded currents for I_{NS} and thus, the I–V relationships for I_{Mn} are similar to those for I_{Ca} (Akaike, Lee & Brown, 1978; Nishi et al., 1983). (3) Increases in $[Mn^{2+}]_o$ augmented I_{Mn} hyperbolically, as already found in the relationship between $[Ca^{2+}]_o$ and I_{Ca} (Akaike, Lee & Brown, 1978). (4) I_{Mn} was blocked by organic or inorganic Ca^{2+} antagonists at concentrations appropriate to block I_{Ca}. (5) I_{Mn} was blocked by the internal perfusion of F^- and reduced by increasing $[Ca^{2+}]_i$.

Increases in concentration of divalent ions such as Ca^{2+}, Ba^{2+} and Sr^{2+} are known to produce shifts in a positive direction in the critical mem-

brane potential for the regenerative responses and also in the *I–V* relationships (Hagiwara & Takahashi, 1967*b*; Blaustein & Goldman, 1968; Okamoto et al., 1976; Akaike, Lee & Brown, 1978; Satow & Kung, 1979). In *Helix* neurons an increase in $[Mn^{2+}]_o$ also produced the shift in the *I–V* relations along the voltage axis. This could be due to the stabilizing action of Mn^{2+} as observed for other divalent cations in the excitable cell membrane. It has been reported that the surface charge of the cell membrane plays an important role in determining ionic selectivity and saturation characteristics of the Ca channel of tunicate eggs (Ohmori & Yoshii, 1977) and mammalian oocytes (Okamoto et al., 1977). If this is the case also in the *Helix* neuron, effects of Mn^{2+} on the surface charge of the *Helix* soma membrane cannot be neglected while analyzing I_{Mn} characteristics. Therefore, we tried to minimize the stabilizing effects of Mn^{2+} on the membrane by adding Mg^{2+}, which would be expected to neutralize the surface charge, since the stabilizing action of Ca^{2+} on the barnacle muscle fiber membrane is abolished by Mg^{2+} at a concentration of 100 mM in the external medium (Hagiwara & Takahashi, 1967*b*). However, even in the presence of high concentrations of Mg^{2+} (40 to 60 mM), the voltage shifts produced by increasing $[Mg^{2+}]_o$ were still observed, even though the shifts were less than in the absence of Mg^{2+}. Higher concentrations of Mg^{2+} than those employed in the present experiments would be required to induce complete neutralization of the surface charge. However, in the *Helix* soma membrane Mg^{2+} at concentrations as high as 100 mM in the external solution produced a progressive reduction of I_{Mn} as well as irreversible changes in membrane activity. Because of the limitation of osmotic pressure of the external solution for *Helix* neurons, a further increase of Mg^{2+} in the external medium would inevitable result in alterations of physical properties of the membrane. Thus, it is impossible to examine the true permeation of Mn^{2+} and other divalent cations under conditions of complete elimination of surface charge effects of respective cations by simply adding Mg^{2+} into the external medium.

Inactivation of I_{Ca} depends on both voltage and $[Ca^{2+}]_i$ accumulation resulting from Ca^{2+} influx through voltage-activated Ca channels, and occurs at two rates, fast and slow with time constants of τ_{h1} and τ_{h2} (Magura, 1977; Akaike, Nishi & Oyama, 1981; Brown et al., 1981). The present experiments have shown that the inactivation process of I_{Ba} and I_{Sr} also show two time constants corresponding to τ_{h1} and τ_{h2} for I_{Ca}, but they are not so distinct as observed for I_{Ca}. However, I_{Mn} and I_{Zn} are inactivated slowly with time constants fitted by a single exponential function. There are at least two possible explanations for the single inactivation time constants of I_{Mn} and I_{Zn}. In a slower activation process the inflection point for fast and slow time courses may become obscure and hence, a current may only appear to be inactivated with a single time constant. In fact, at low voltage steps (−20 to −10 mV) where activation of the I_{Ca} was slow, τ_{h1} for I_{Ca} became larger and the inflection point for differentiating the time course of inactivation of the I_{Ca} is not clear. Alternatively, the inactivation process of currents carried through Ca channels may consist of only a single component with a slow time constant, as observed for I_{Mn} or I_{Zn}. Support for this explanation comes from our recent preliminary studies on I_{Ca} in which we have observed that τ_{h1} for I_{Ca} becomes larger with prolonged internal perfusion of the cell with a solution containing EGTA and caffeine and τ_{h1} becomes closer to τ_{h2}. It is in this connection that further characterization of I_{Ca} inactivation is now under way.

Thus, the present experiments not only provided direct evidence that Mn^{2+} as well as other divalent cations pass through Ca channels in the *Helix* soma membrane, but also further insight into the general characteristics of the Ca channel.

We wish to thank Drs. C. Edwards, D. Carpenter and S.K. Sikdar for their helpful advice on the manuscript. This work was supported partially by a grant from Tanabe Pharmaceutical Company, Japan.

References

Adams, D.J., Gage, P.W. 1979. Characteristics of sodium and calcium conductance change produced by membrane depolarization in an *Aplysia* neurone. *J. Physiol. (London)* **289**:143–162

Akaike, N. 1980. Internal perfusion of single cell by suction electrode. *Seitainokagaku* **31**:55–71

Akaike, N., Brown, A.M., Nishi, K., Tsuda, Y. 1981. Actions of verapamil, diltiazem and other divalent cations on the calcium-current of *Helix* neurones. *Br. J. Pharmacol.* **74**:87–95

Akaike, N., Fishman, H.M., Lee, K.S., Moore, L.E., Brown, A.M. 1978. The units of calcium conductance in *Helix* neurones. *Nature (London)* **247**:379–382

Akaike, N., Lee, K.S., Brown, A.M. 1978. The calcium current of *Helix* neurone. *J. Gen. Physiol.* **71**:509–531

Akaike, N., Nishi, K., Oyama, Y. 1981. The Manganese Current of *Helix* Neuron. The Mechanism of Gated Calcium Transport Across Biological Membranes. p. 111–117. Academic Press, New York

Anderson, P.A.V. 1979. Epithelial conduction in salps. *J. Exp. Biol.* **80**:231–239

Blautstein, M.P., Goldman, D.E. 1968. The action of certain polyvalent cations on voltage clamped lobster axons. *J. Gen. Physiol.* **51**:279–291

Brown, A.M., Morimoto, K., Tsuda, Y., Wilson, D.L. 1981. Calcium current-dependent and voltage-dependent inactivation of calcium channels in *Helix aspersa*. *J. Physiol. (London)* **320**:193–218

Byerly, L., Hagiwara, S. 1982. Calcium currents in internally perfused nerve cell bodies of *Limnea stagnalis*. *J. Physiol. (London)* **322**:503–528

Connor, J.A., Stevens, C.F. 1971. Voltage clamp studies of a transient outward membrane current in gastropod neural somata. *J. Physiol. (London)* **213**:21–30

Frankenhaeuser, B., Hodgkin, A.L. 1957. The action of calcium on the electrical properties of squid axons. *J. Physiol. (London)* **137**:218–244

Fukuda, J., Kawa, K. 1977. Permeation of manganese, cadmium, zinc, beryllium through calcium channels of an insect muscle membrane. *Science* **196**:309–311

Geduldig, D., Gruener, R. 1970. Voltage clamp of the *Aplysia* giant neurone: Early sodium and calcium currents. *J. Physiol. (London)* **211**:217–244

Hagiwara, S., Miyazaki, S. 1977. Ca and Na spikes in egg cell membrane. *Prog. Clin. Biol. Res.* **15**:147–158

Hagiwara, S., Takahashi, K. 1967*a*. Resting and spike potentials of skeletal muscle fibers of salt-water elasmobranch and teleost fish. *J. Physiol. (London)* **190**:499–518

Hagiwara, S., Takahashi, K. 1967*b*. Surface density of calcium ions and calcium spikes in the barnacle muscle fiber membrane. *J. Gen. Physiol.* **50**:583–601

Hodgkin, A.L., Huxley, A.F. 1952. A quantitative description of membrane current and its application to conduction and excitation in nerve. *J. Physiol. (London)* **177**:500–544

Kawa, K. 1979. Zinc-dependent action potentials in giant neurons of the snail, *Euhadra quaestia*. *J. Membrane Biol.* **49**:325–344

Kerkut, G.A., Lambert, J.D.C., Gayton, R.J., Loker, J.E., Walker, R.J. 1975. Mapping of nerve cells in the subesophageal ganglia of *Helix aspersa*. *Comp. Biochem. Physiol.* **50**:1–25

Kostyuk, P.G. 1980. Calcium ionic channels in electrically excitable membrane. *Neuroscience* **5**:945–959

Kostyuk, P.G., Krishtal, O.A., Pidoplichko, V.I. 1975. Effect of internal fluoride and phosphate on membrane currents during intracellular dialysis of nerve cells. *Nature (London)* **257**:691–693

Kostyuk, P.G., Krishtal, O.A., Shakhovalov, Y.A. 1977. Separation of sodium and calcium currents in the somatic membrane of molluscan neurones. *J. Physiol. (London)* **270**:545–568

Lee, K.A., Akaike, N., Brown, A.M. 1977. Trypsin inhibits the action of tetrodotoxin on neurones. *Nature (London)* **265**:751–753

Lee, K.S., Akaike, N., Brown, A.M. 1980. The suction pipette method for internal perfusion and voltage clamp of small excitable cells. *J. Neurosci. Meth.* **2**:51–78

Magura, I.S. 1977. Long-lasting inward current in snail neurons in barium solutions in voltage-clamp conditions. *J. Membrane Biol.* **35**:239–256

Nishi, K., Akaike, N., Oyama, Y., Ito, H. 1983. Characteristics of calcium currents and actions of calcium-antagonists on calcium and potassium currents in the *Helix* neurones: Their specificity and potency. *Circ. Res.* **52 (Suppl. I)**:53–59

Ochi, R. 1970. The slow inward current and the action of manganese ions in guinea-pig's myocardium. *Pfluegers Arch.* **316**:81–94

Ochi, R. 1976. Manganese-dependent propagated action potentials and their depression by electrical stimulation in guinea-pig myocardium perfused by sodium-free media. *J. Physiol. (London)* **263**:139–156

Ohmori, H., Yoshii, M. 1977. Surface potential reflected in both gating and permeation mechanisms of sodium and calcium channels of the tunicate egg cell membrane. *J. Physiol. (London)* **267**:429–463

Okamoto, H., Takahashi, K., Yamashita, N. 1977. Ionic currents through the membrane of the mammalian oocyte and their comparison with those in the tunicate and sea urchin. *J. Physiol. (London)* **267**:465–495

Okamoto, H., Takahashi, K., Yoshii, M. 1976. Two components of the calcium current in the egg cell membrane of the tunicate. *J. Physiol. (London)* **255**:527–561

Oyama, Y., Nishi, K., Yatani, A., Akaike, N. 1982. Zinc current in *Helix* soma membrane. *Comp. Biochem. Physiol.* **72**:403–410

Palade, P.T., Almers, W. 1978. Slow Na and Ca currents across the membrane of frog skeletal muscle fibers. *Biophys. J.* **21**:168*a*

Satow, Y., Kung, C. 1979. Voltage sensitive Ca-channels and the transient inward current in *Paramecium tetraurelia*. *J. Exp. Biol.* **78**:149–161

Takahashi, K., Yoshii, M. 1978. Effects of internal free calcium upon the sodium and calcium channels in the tunicate egg analyzed by the internal perfusion technique. *J. Physiol. (London)* **279**:519–549

Thompson, S.H. 1977. Three pharmacologically distinct potassium channels in molluscan neurones. *J. Physiol. (London)* **265**:465–488

Yamagishi, S. 1973. Manganese-dependent action potentials in intracellularly perfused squid giant axons. *Proc. Jpn. Acad.* **49**:218–222

Received 18 January 1983, revised 12 May 1983